

# The average longitudinal air shower profile: exploring the shape information

R. Conceição<sup>1</sup>, S. Andringa<sup>1</sup>, F. Diogo<sup>1</sup>, M. Pimenta<sup>1,2</sup>

<sup>1</sup> LIP, Av. Elias Garcia, 14-1, 1000-149 Lisboa, Portugal

<sup>2</sup> Departamento de Física, IST, Av. Rovisco Pais, 1049-001 Lisboa, Portugal

E-mail: [ruben@lip.pt](mailto:ruben@lip.pt)

**Abstract.** The shape of the extensive air shower (EAS) longitudinal profile contains information about the nature of the primary cosmic ray. However, with the current detection capabilities, the assessment of this quantity in an event-by-event basis is still very challenging. In this work we show that the average longitudinal profile can be used to characterise the average behaviour of high energy cosmic rays. Using the concept of universal shower profile it is possible to describe the shape of the average profile in terms of two variables, which can be already measured by the current experiments. These variables present sensitivity to both average primary mass composition and to hadronic interaction properties in shower development. We demonstrate that the shape of the average muon production depth profile can be explored in the same way as the electromagnetic profile having a higher power of discrimination for the state of the art hadronic interaction models. The combination of the shape variables of both profiles provides a new powerful test to the existing hadronic interaction models, and may also provide important hints about multi-particle production at the highest energies.

## 1. Introduction

The origin and nature of ultra high energy cosmic rays (UHECRs) is still unknown. Although it is expected to be of hadronic nature, something between proton and iron, the determination of the UHECRs mass composition is still one of the present biggest challenges on the experiments dedicated to the study of these particles. Their mass composition can only be inferred indirectly through the analysis of the shower that was initiated by the interaction of UHECRs with the atmosphere atoms.

However, the shower development depends also on the hadronic interactions for which there is no first principle description, only different phenomenological models that try to extrapolate the accelerator data obtained at lower energies and different phase space regions.

The analysis of the electromagnetic (e.m.) shower longitudinal profile can be used to determine the primary energy and composition. The primary energy is related with the maximum number of particle,  $N_{max}$ , and the primary mass composition can be inferred statistically from the depth at which the maximum occurs,  $X_{max}$ . Again, this mass composition observable has also a strong dependence on the primary cross-section. There is, however, more information hidden in the details of the shower longitudinal profile shape [1, 2, 3].

Electromagnetic longitudinal shower profiles are well described by the Gaisser-Hillas function,



which can be parametrised in  $N' \equiv N/N_{max}$  and  $X' \equiv X - X_{max}$  as:

$$N' = \left(1 + \frac{RX'}{L}\right)^{R-2} \exp\left(-\frac{X'}{LR}\right) \quad (1)$$

With the above parametrisation, introduced in [1], the profile can be recognised as a Gaussian, of width  $\mathbf{L}$ , with an asymmetry introduced by non-zero values of  $\mathbf{R}$ . It is worth noting that after translating the maximum to zero all the variations due to the point of the first interaction disappear. In other words, the shape should be insensitive to the primary cross-section.

The shape of the electromagnetic longitudinal profile has been shown to be sensitive to primary mass composition, in an event-by-event basis, using simulated showers [1]. However, from the experimental point of view this is not an easy measurement. The Gaisser-Hillas fit to extract the shape parameters is affected by the statistical uncertainties on the light collection by the fluorescence telescopes and the uncertainty on the determination of  $X_{max}$ . Moreover, this kind of optical experiments have several systematic uncertainties such as Cherenkov direct and scattered light estimation, telescope alignment, atmospheric conditions, among others [4, 5]. This makes it extremely difficult to extract the information on the shape, in particular to access the two shape parameters at the same time (see fig. 1 (left)).

A possible strategy would be to look at the average longitudinal profile taking advantage of its universal behaviour, as shown in figure 1 (right). By doing so, the statistical uncertainties should be reduced, so that the two shape parameters,  $\mathbf{L}$  and  $\mathbf{R}$ , can be fit simultaneously. On the other hand, the measurement of the average profile could help to control the experimental systematic uncertainties enabling future event-by-event analysis (for instance, the results between different telescopes should be statistically consistent).

However, such strategies rely on the assumption that the average *universal* electromagnetic longitudinal shower profile still has information about the primary mass composition.

To investigate this, we have generated, using CONEX [6, 7], 10000 showers of proton, helium, nitrogen and iron, for different hadronic interaction models (SIBYLL2.1 [8], QGSJET-II.04 [9] and EPOS-LHC [10, 11]) and different energies being the reference energy through this manuscript  $E = 10^{19}$  eV. The zenith angle was fixed at  $40^\circ$  as it was shown previously [1, 12] that the shape do not depends significantly on this quantity.

The first test that one can conceive is to average several electromagnetic shower profiles and then extract the two shape variable through a Gaisser-Hillas fit using equation (1). The fit range was chosen as  $X' \in [-300; 200]\text{gcm}^{-2}$ . Although the choice of the fit range is somewhat arbitrary, it had as motivation the experimental conditions at which the measurement should be done: on one hand include a range as big as possible to increase the significance of the fit procedure; on the other hand exclude regions such as the tails where the uncertainties are large, for instance due to the Cherenkov scattering light component. The proposed test is shown in figure 2 for different primaries and as a function of the number of events that was used to perform the average.

It can be seen from this figure that in fact, the average e.m. profile is sensitive to the difference between primaries. Moreover, the values of  $\mathbf{L}$  and  $\mathbf{R}$  converge after averaging a few hundred events allowing to distinguish between the different primaries. Another important point to make is that, as expected, both shape parameters contain relevant information about the primary particle.

In the following sections we shall explore the sensitivity of the shape of the longitudinal profile to both primary mass composition and hadronic interaction models. In section 3 we will discuss the same for the average muon production depth profile. Finally, we end with some conclusions.

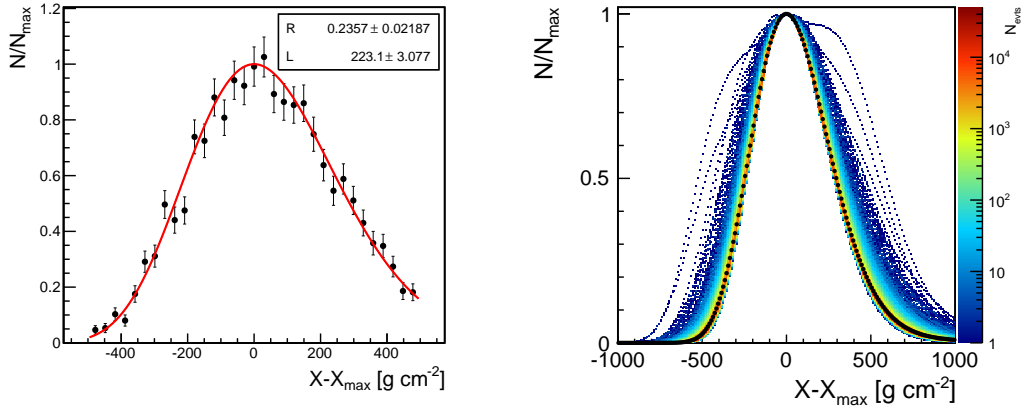


**Figure 1.** (left) Single electromagnetic longitudinal profile written as a function of  $X' \equiv X - X_{max}$  and normalized to its maximum,  $N_{max}$ . The error bars represent the statistical uncertainty for a typical UHECR shower event measured by a fluorescence telescope. (right) The black points represent the average electromagnetic longitudinal profile averaged over the 10000 shower profiles displayed in the plot. The color code represents the density of showers in  $(X', N')$ .

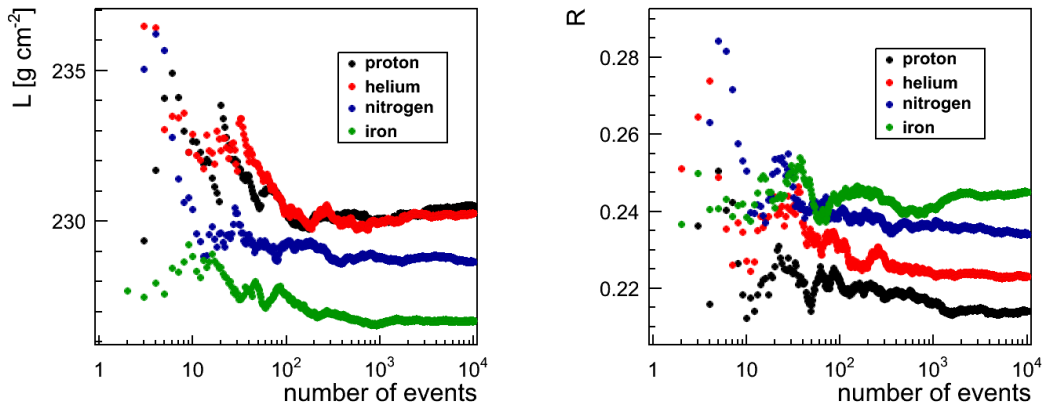


**Figure 2.** Shape parameters  $L$  (left) and  $R$  (right) as a function of the number of events used to get the average shower. The showers were generated using QGSJET-II.04 as the high energy hadronic interaction model. Color codes show different primaries at  $\log(E/\text{eV}) = 19.0$ .

## 2. Average electromagnetic profile shape

In this section we shall discuss the properties that can be extracted from the shape of the average electromagnetic profile.

### 2.1. Sensitivity to primary mass composition

It has been seen in the previous section that the average longitudinal electromagnetic shape variables  $L$  and  $R$  are both sensitive to the nature of the cosmic ray that induces the shower. It is then only natural to plot both variables at the same time to assess its sensitivity to the primary mass composition. This is what is shown in figure 3. The crosses represent the

values ( $\mathbf{L}, \mathbf{R}$ ) for pure mass composition samples. In this figure it is also shown all the possible mass composition possibilities using four primaries: proton, helium, nitrogen and iron. Each coloured dot represents a particular mass composition scenario and the colour is the average mass logarithm given by,

$$\langle \ln(A) \rangle = f_p \ln(1) + f_{He} \ln(4) + f_N \ln(14) + f_{Fe} \ln(56) \quad (2)$$

where  $f_X$  is the fraction of the element  $X$ .

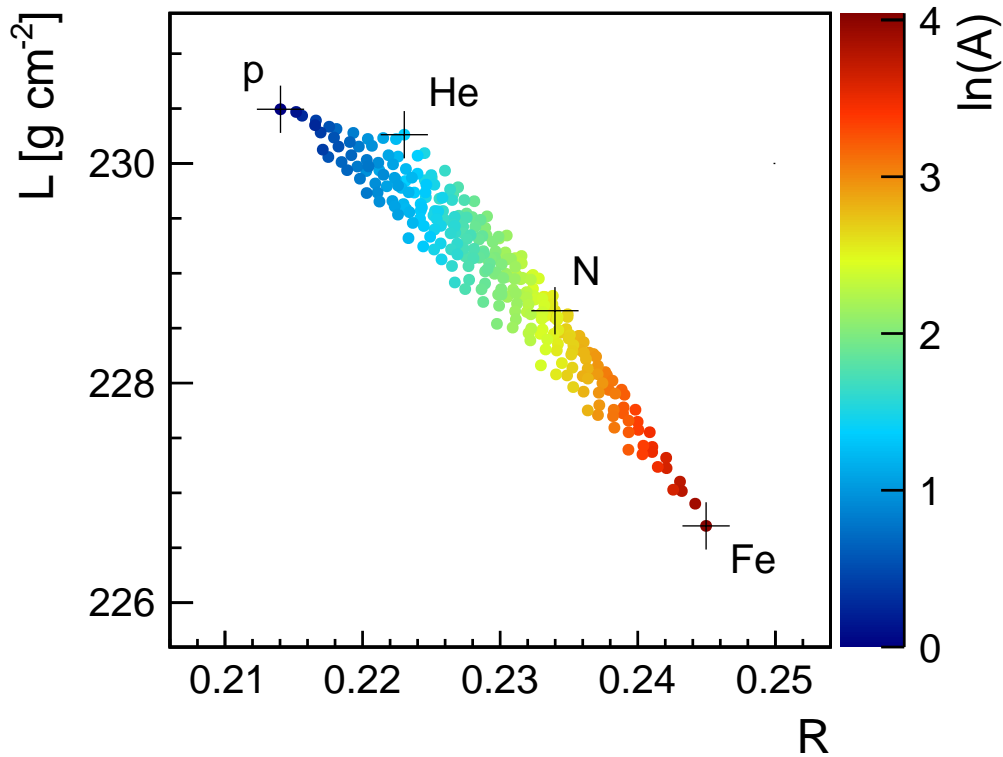


**Figure 3.** Relation of the shape parameters of the average shower profile with the  $\langle \ln(A) \rangle$ . The showers were generated using QGSJET-II.04 at  $\log(E/\text{eV}) = 19$ . Color codes show the  $\langle \ln(A) \rangle$  for different combinations of primaries and crosses mark the results for pure composition samples. Each point was generated averaging 10000 shower longitudinal profiles.

It is possible to conclude from this figure that, within a particular hadronic interaction model, the assessment of the shape quantities  $\mathbf{R}$  and  $\mathbf{L}$  can be used to derive the  $\langle \ln(A) \rangle$ , similar to what is done for  $X_{max}$  [13], independently of the first interaction point.

## 2.2. Sensitivity to Hadronic Interaction Models

The dependence of the shape variables with the hadronic interaction models was also investigated. It can be seen, in figure 4 that there is some discrimination power for the standard hadronic interaction models. Although EPOS-LHC and QGSJET-II.04 have some overlap there are some mass composition choices for which the models occupy a different phase space, for instance for pure proton.

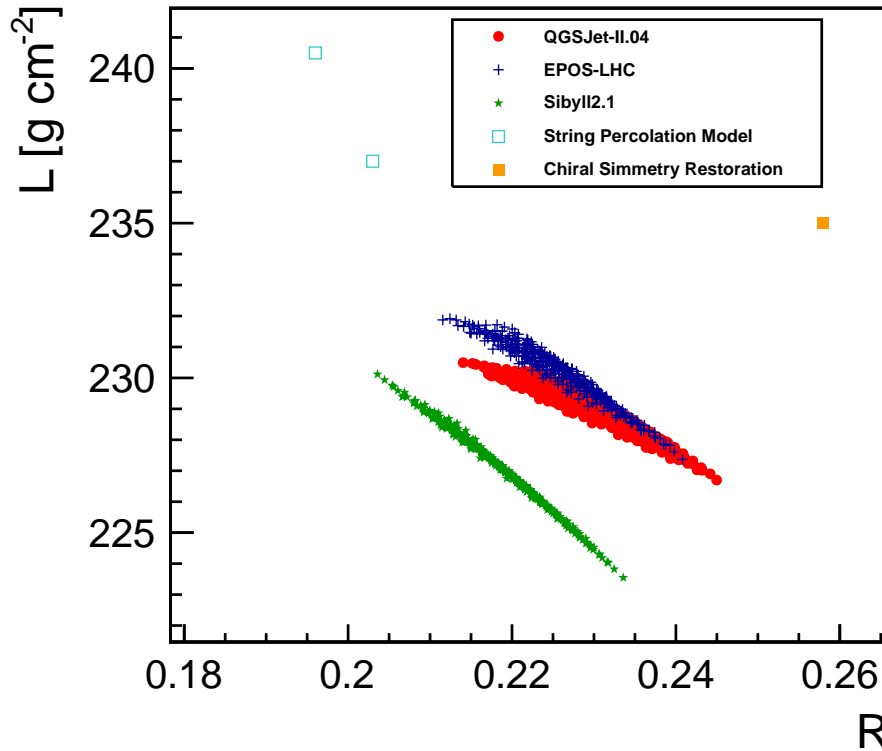


**Figure 4.** Shape parameters (**L**, **R**) of the average electromagnetic shower profile, generated at  $\log(E/\text{eV}) = 19$ , for the different mass composition combinations with different hadronic interaction models (see legend for details).

The predictions for the shape variables of the e.m. average profile from exotic models (models that try to explain the UHECR data through changes on the hadronic interaction physics while the mass composition remains constant) are also displayed on fig. 4. It can be seen from this plot that the shape variables have a strong discrimination power for this kind of models. Moreover, note that these models were tuned to reproduce the  $X_{max}$  and the number of muons at ground. Therefore, the measurement of the shape of the average electromagnetic profile is an important test to this exotic scenarios.

The energy evolution of the shape variables phase space for different models was also investigated and is presented in figure 5 (for all the available high energy hadronic interaction models, including older versions). All the models display a similar behaviour: as the energy increases **L** increases and **R** decreases. The increase of **L** is explained by its relation with the shower energy (remember that **L** is the width of the gaussian, and therefore related with the integral which by its turn gives the energy). On the other hand, the decrease of **R** is an indication that the shower is getting less asymmetrical (more gaussian). Moreover, the distance between the models phase space is being reduced as the energy increases. This may be an indication that the shower is becoming more universal and that the difference between models have a lower impact on the shower development. Finally, it is worth to mention that the newer versions of the models seems to be favouring higher **L** and **R** parameters. These models have been re-tuned not only to describe better the new Large Hadron Collider (LHC) data but also to reproduce

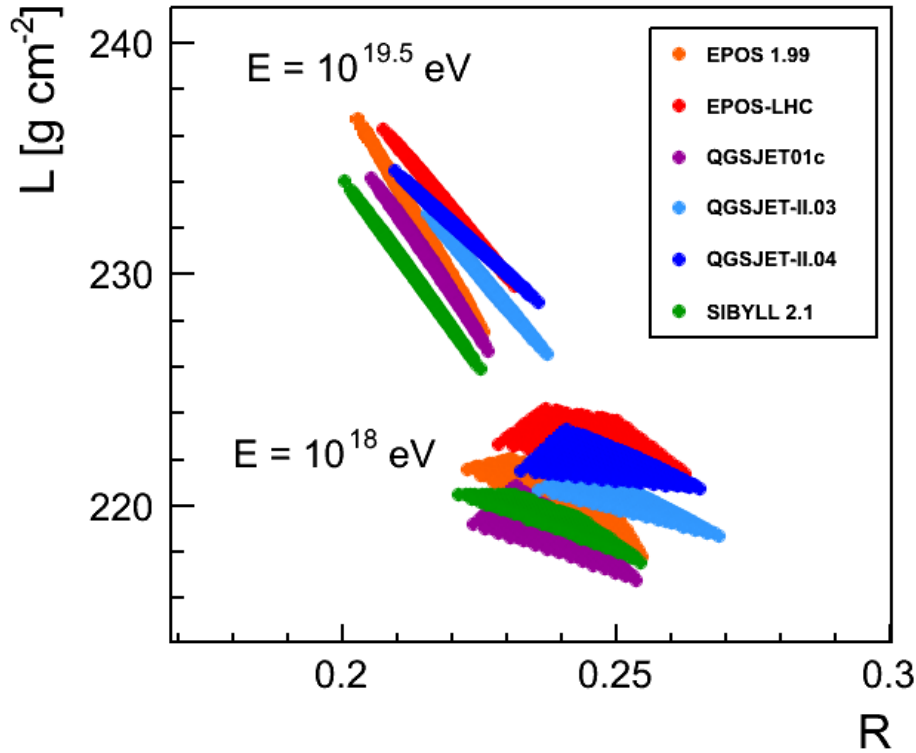


**Figure 5.** Shape parameters ( $L$ ,  $R$ ) of the average electromagnetic shower profile for the different mass composition combinations with different hadronic interaction models (see legend for details). The results are shown for two different energies:  $\log(E/\text{eV}) = 18$  (bottom) and  $\log(E/\text{eV}) = 19.5$  (top).

the number of muons at ground measured by UHECR experiments. The increase of the muon content on simulated showers affects the balance between the electromagnetic and hadronic shower component and this should be reflected in the shower average longitudinal shape. This means that the assessment of the  $L$  and  $R$  of the average profile may be used to evaluate some of the tunings of the hadronic interaction models.

### 3. Average muon production depth profile shape

It has been shown in [12] that the muon production depth profile also presents an universal shape when presented in terms of  $X' = X - X_{max}^\mu$  and  $N' = N/N_{max}$ . Moreover it has been shown in this same manuscript that this profile can be describe by a Gaisser-Hillas function and its main characteristics ( $X_{max}$  and shape) have the same sensitivity to mass composition and hadronic physics as the ones from the electromagnetic profile.

Hence, it is only natural that the previous investigations on the electromagnetic shower average profile are now applied to the muon production depth *average* profile. The results of this investigation can be summarised in figure 6. In this plot we show the shape variables of the average muon production depth profile for three different hadronic interaction models. Similarly, to what was shown for the e.m. profile in fig. 4, each point represents a specific mass composition combination of p, He, N and Fe, and the full area displays the possible phase space within a

model.

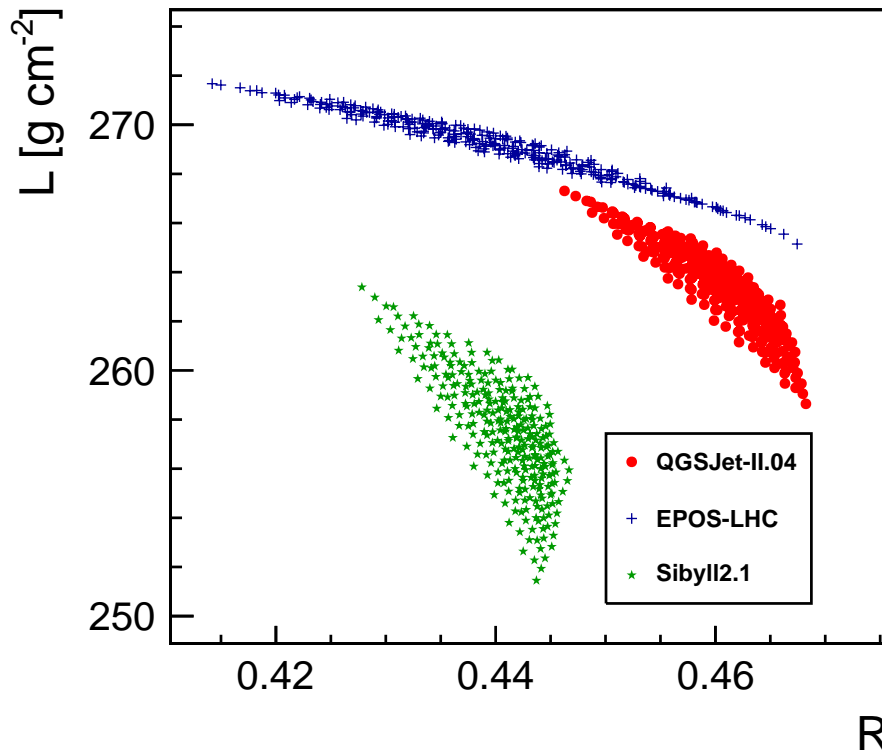


**Figure 6.** Shape parameters ( $L$ ,  $R$ ) of the average muon production depth profile, generated at  $\log(E/\text{eV}) = 19$ , for the different mass composition combinations with different hadronic interaction models (see legend for details).

It is clear from this plot that for all the models, both muonic shape variables have higher values than the ones from the electromagnetic profile, which means that the muonic production profile is broader and more asymmetric. A closer inspection of the plot reveals that the shape variables of this profile have a higher power of discrimination between models than the ones from the e.m. profile. In fact, the models can be distinguished independently of the primary mass composition. However, presently, this profile is more difficult to measure experimentally [14].

Finally, it is important to emphasise that the assessment of the electromagnetic and muonic profile gives insight to distinct components of the shower. The former is related to  $\pi^0$  production and to the development of the electromagnetic cascade (photons, electrons...), which decouples very early from hadronic shower development, while the later arises essentially from the decay of charged pions and kaons being thus sensitive to all the stages of the hadronic shower.

Although these two profiles may give insight to different processes and stages of the shower development, both are connected by the same primary particle. This means that the interpretation of the shower observables, in particular the shape variables of the average profiles, need to present consistent results in terms of primary mass composition. The failure to achieve this would be a proof that there are inconsistencies with the shower description. Hence, a combined analysis of figures 4 and 6 can enhance our capability to test our knowledge over hadronic interaction models (or other exotic models) independently of the primary mass

composition.

#### 4. Conclusions

The interpretation of UHECRs in terms of mass composition is bounded to our understanding of hadronic interactions at the highest energies. It has been shown that the shape of the shower profile provides a new insight over shower mass composition and hadronic interaction physics without depending on the first interaction. Although very promising, these quantities are not easy to access experimentally on an event-by-event basis. Hence, in this work we propose to measure instead the shape of the *average* electromagnetic shower profile. In this way one could measure simultaneously the two shape parameters. We have demonstrated that the shape of the average electromagnetic longitudinal profile is both sensitive to mass composition and to hadronic interaction models. Moreover, we have investigated the shape of the muon production depth profile, using the same procedure, and obtained similar findings. In fact, the shape the average muon production profile allow us to discriminate between hadronic interaction models independently of the considered mass composition. Finally, it is important to note that not only the shape of these two distinct average profiles are offering different insights of the shower development, but they are also bounded to the same primary. Therefore, a combined analysis can provide strong tests to our current knowledge over the shower description by requiring that the shapes of the two profiles are interpreted in terms of the same primary mass composition.

#### Acknowledgments

This work is partially funded by Fundação para a Ciência e Tecnologia (SFRH/BPD/73270/2010) and (SFRH/BD/89109/2012).

#### References

- [1] Andringa S, Conceição R and Pimenta M 2011 *Astropart.Phys.* **34** 360–367
- [2] Matthews J, Mesler R, Becker B, Gold M and Hague J 2010 *J.Phys.G* **G37** 025202 (*Preprint* 0909.4014)
- [3] Giller M, Kacperczyk A, Malinowski J, Tkaczyk W and Wieczorek G 2005 *J.Phys.G* **G31** 947–958
- [4] Keilhauer B, Bohacova M, Fraga M, Matthews J, Sakaki N *et al.* 2013 *EPJ Web Conf.* **53** 01010 (*Preprint* 1210.1319)
- [5] Pekala J, Homola P, Wilczynska B and Wilczynski H 2009 *Nucl.Instrum.Meth.* **A605** 388–398 (*Preprint* 0904.3230)
- [6] Pierog T *et al.* 2006 *Nucl. Phys. Proc. Suppl.* **151** 159–162 (*Preprint* astro-ph/0411260)
- [7] Bergmann T *et al.* 2007 *Astropart. Phys.* **26** 420–432 (*Preprint* astro-ph/0606564)
- [8] Ahn E J, Engel R, Gaisser T K, Lipari P and Stanev T 2009 *Phys.Rev.* **D80** 094003 (*Preprint* 0906.4113)
- [9] Ostapchenko S 2011 *Phys.Rev.* **D83** 014018 (*Preprint* 1010.1869)
- [10] Werner K, Liu F M and Pierog T 2006 *Phys.Rev.* **C74** 044902 (*Preprint* hep-ph/0506232)
- [11] Pierog T, Karpenko I, Katzy J, Yatsenko E and Werner K 2013 (*Preprint* 1306.0121)
- [12] Andringa S, Cazon L, Conceição R and Pimenta M 2012 *Astropart.Phys.* **35** 821–827 (*Preprint* 1111.1424)
- [13] Kampert K H and Unger M 2012 *Astropart.Phys.* **35** 660–678 (*Preprint* 1201.0018)
- [14] Cazon L, Conceição R, Pimenta M and Santos E 2012 *Astropart.Phys.* **36** 211–223 (*Preprint* 1201.5294)